J. Astron. Space Sci. 25(4), 335–346 (2008)

Seasonal Characteristics of the Longitudinal Wavenumber-4 Structure in the Equatorial Ionospheric Anomaly

E. Kim[1], G. Jee[2], and Y. H. Kim[1†]
[1]Department of Astronomy and Space Science, Chungnam National University, Daejeon, Korea
[2] Korea Polar Research Institute, KORDI, Incheon, Korea
email: jinastro@cnu.ac.kr, ghjee@kopri.re.kr, yhkim@cnu.ac.kr

(Received September 18, 2008; Accepted October 21, 2008)

Abstract

Using the global total electron contents (TEC) measured by the TOPEX satellite from Aug. 1992 to Oct. 2005, we investigate the variations of the longitudinal wavenumber-4 (LW-4) structure in the equatorial anomaly (EA) crests with season, local time, and solar activity. Our study shows that the LW-4 structure in the EA crests (5~20° MLAT in both hemispheres) has clear four peaks at fixed longitude sectors during the daytime for both equinoxes and June solstice. In spite of being called a wavelike structure, however, the magnitudes and spatial intervals of the four peaks are far from being the same or regular. After sunset, the four-peak structure begins to move eastward with gradual weakening in its amplitude during equinoxes and this weakening proceeds much faster during June solstice. Interestingly, the longitudinal variations during December solstice do not show clear four-peak structure. All these features of the LW-4 structure are almost the same for both low and high solar activity conditions although the ion densities are greatly enhanced from low to high solar activities. With the irrelevancy of the magnetic activity in the LW-4, this implies that the large changes of the upper atmospheric ion densities, one of the important factors for ion-neutral interactions, have little effect on the formation of the LW-4 structure. On the other hand, we found that the monthly variation of the LW-4 is remarkably similar to that of the zonal component of wavenumber-3 diurnal tides at low latitudes, which implies that the lower atmospheric tidal forcing, transferred to the upper atmosphere, seems to have a dominant role in producing the LW-4 structure in the EA crests via the E-region dynamo.

Keywords: equatorial ionosphere, equatorial anomaly, total electron content (TEC), tidal winds, upper and lower atmospheres coupling

1. Introduction

Recently it was revealed that the equatorial anomaly (EA) crests show the longitudinal wavenum ber-4 (LW-4) structure when they are presented in the latitude and longitude coordinates for a fixed

†corresponding author

local time. This longitudinal structure was first reported in Sagawa et al. (2005) in a global distribution map of nightglow emission intensities for a fixed local time interval, obtained from the Far Ultraviolet Imager (FUV) on board the IMAGE satellite from March to June 2002. In their constant local time map of the nightglow, peaks and dips of the EA crests have about 90° longitudinal separations in the longitude range from 0° to 250°. They noticed that the EA longitudinal variation can be regarded as a wavenumber-4 structure. After examining possible factors causing longitudinal variations of the ionosphere, such as the difference between geomagnetic and geographic equators, the declination angle, and electric and magnetic field variations, they concluded that all these factors couldn't explain their observational results and proposed a forcing from below, specifically non-migrating tides, as a possible candidate for explaining the longitudinal wavenumber-4 (LW-4) structure. This structure was then further reported and discussed in several studies using various observations and modeling studies for the equatorial ionosphere including Immel et al. (2006), England et al. (2006a,b), Hartman & Heelis (2007), Kil et al. (2007), Lin et al. (2007), Oh (2007), Scherliess et al. (2008).

During the daytime, the E-region dynamo electric field resulting from the migrating diurnal tide can be modified by the additional lower atmospheric forcing that is initiated from the eastward propagating diurnal tide with zonal wave number 3. This non-migrating tide (DE3) is primarily excited by latent heat release in the tropical troposphere associated with the raindrop formation in deep convective clouds and intimately connected with the predominant wavenumber-4 longitude distribution of topography and land-sea difference at low latitudes (Zhang et al. 2006, Forbes et al. 2006). The resulting modified E-region dynamo electric field produces a similar longitudinal wavenumber-4 structure of the F-region equatorial $E \times B$ ion drifts in a fixed local time frame, which results in the LW-4 structure of the EA crests and crest latitudes (Immel et al. 2006, England et al. 2006a,b). Although the specific physical mechanism for this structure has not been established, a brief explanation can be found in Kil et al. (2007); the background dawn-to-dusk dynamo electric field can be enhanced or reduced by the additional polarization electric fields that are induced, in alternate directions, from the opposite charge accumulations at the crests and troughs of the non-migrating tidal winds.

Most of the previous studies on the LW-4 have been focused on its existence in the ionosphere mainly during equinoxes, and on the possible relation with the non-migrating tides from the lower atmosphere. In particular, Scherliess et al. (2008) utilized the 13-year total electron content (TEC) measurements from the TOPEX/Poseidon mission to investigate the longitudinal variability (in particular, the LW-4 structure) of the low-latitude ionosphere with local time, season, solar and geomagnetic activities. It was found in their climatological study that the LW-4 is almost independent of the solar and geomagnetic activities but shows noticeable variations with season and local time. Major results found in their study are as follows. The LW-4 structure is created during equinoxes and June solstice but it is absent, or washed out by other processes, during December solstice. This structure is largely independent of the solar activity and also observed during geomagnetically active conditions as well as the quiet conditions. During June solstice, the LW-4 structure is observed in the afternoon hours but, in contrast to the equinox cases, it exhibits a strong hemispheric asymmetry and is not observed during the night. Forbes et al. (1996) and Vladimer et al. (1999) have also used the TOPEX TEC measurements to study longitudinal structure of the F-region ionosphere. Particularly, Vladimer et al. (1999) observed a relative maximum TEC value of the EA in the Indian/Asian longitude sector with a relative TEC decrease in the western American region, but the complete LW-4 structure was not identified. By utilizing the same TOPEX TEC measurements, we will further investigate the LW-4 structure with an emphasis on its seasonal characteristics for different local times and solar activities. From the analysis, we will discuss the associations of the LW-4 structure with

both the lower atmospheric tidal forcing and the upper atmospheric ion densities. In the following sections, we will describe the data and analysis for our study and then discuss the resulting seasonal characteristics of the LW-4 structure. Finally, the summary and conclusion will be presented.

2. TOPEX TEC Measurements

The TOPEX satellite measured the TEC over the oceans for more than a solar cycle, and thus provided good complementary TEC data to the conventional TEC measurements such as the GPS TEC data (Fu et al. 1994, Ho et al. 1997, Codrescu et al. 1999, 2001, Lynn et al. 2004, Jee et al. 2004, 2005, Zhu et al. 2006, Horvath 2006). In this section only brief introduction for the TOPEX TEC measurements will be given and the details of the TOPEX/Poseidon mission can be found in the previous studies including Fu et al. (1994) and Jee et al. (2004). The TOPEX TEC measurements were obtained from the joint mission of the National Aeronautics and Space Administration (NASA) and the French space agency, Centre National d'Etudes Spatiales (CNES), which was launched on 10 August 1992 and maintained for about 13 years until October 2005. The satellite of the mission carried for the first time a dual-frequency radar altimeter operating at 13.6 GHz (Ku band) and 5.3 GHz (C band) simultaneously. In order to remove the ionospheric delay imposed on the altimeter, it estimates the electron content along the ray path from the satellite to the sea surface by measuring the travel times of the radio waves at two frequencies. The obtained electron content is equivalent to the TEC of the ionosphere in a column extending from the satellite to the subsatellite reflection point on the surface of the ocean. The TOPEX satellite was orbiting the Earth at an altitude of 1336 km with an inclination angle of 66° and a period of 112 min. The orbit was close to sun-synchronous, advancing by 2° per day, and it therefore takes about 90 days to cover all local times, considering both ascending and descending nodes. The TEC measurements were taken almost every second for about 13 years from the launch on August 1992 until the end of mission on October 2005. The original data were obtained from the NASA Physical Oceanography Distributed Active Archive center at the Jet Propulsion Laboratory (JPL PO.DAAC/NASA) and then averaged for each 18 sec or about 1° of orbit along the satellite orbit. The resulting 18-sec averaged data cover much more than a full solar cycle through the part of cycle 22 to cycle 23 (Fig. 1).

3. Data Analysis

Scherliess et al. (2008) performed quite an extensive climatological study on the LW-4 structure by binning the data with local time, season, solar cycle and geomagnetic activity. Since our study will be focused on the seasonal variabilities of the LW-4 structure with local time and solar activity, the data were binned with local time, season, and solar activity. The geomagnetic activity bins are not included in this study. Jee et al. (2004) performed an extensive study on the climatology of the ionosphere using the TOPEX TEC measurements and reported that TEC values over the EA region show very little variations with the geomagnetic activity. Furthermore, Scherliess et al. (2008) showed that the LW-4 structure is observed during geomagnetically disturbed conditions as well as during quiet conditions, implying that the physical processes causing the LW-4 are present regardless of the geomagnetic conditions. Therefore it can be assumed that the LW-4 structure is largely independent of the geomagnetic activity at least in the climatological ionosphere.

Initially, the TEC maps were produced in the geomagnetic latitude (MLAT) and geographic longitude (GLON) coordinate with the spatial resolution of $2° \times 5°$ in MLAT and GLON for a given magnetic local time (MLT) interval, season, and solar activity, which are defined as follows. First

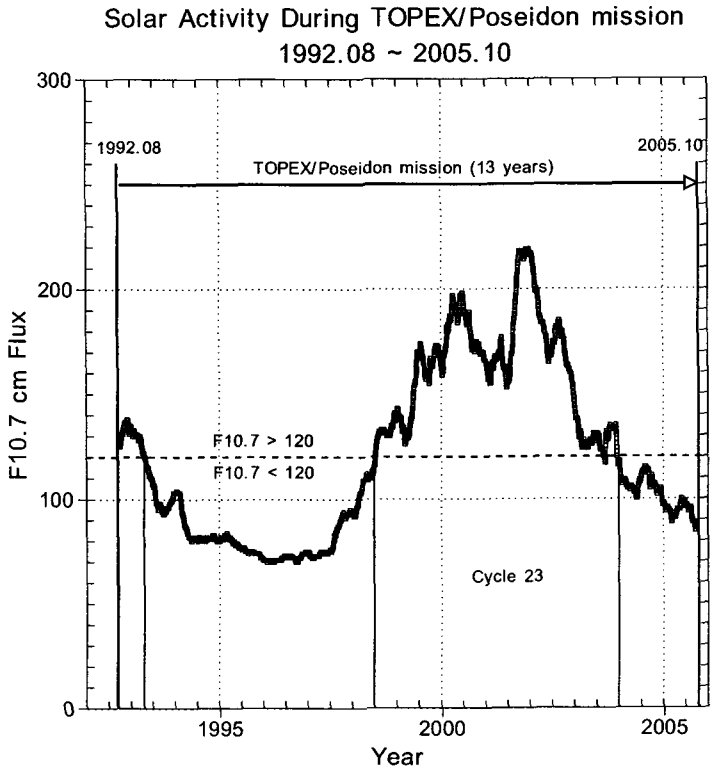

Figure 1. Solar activity (F10.7 cm flux) during the TOPEX/Poseidon mission (August 1992 ~ October 2005). Low and high solar activities are separated with a horizontal dashed line at F10.7 = 120.

of all, the solar activity was binned into low (F10.7 < 120) and high (F10.7 > 120) solar activity conditions as shown in Fig. 1.

For both solar activities, the data are divided into four 3-month seasonal cases: March equinox (March-May), June solstice (June-August), September equinox (September-November), and December solstice (December-February). For each seasonal case, the magnetic local times were binned in every two hours from 08 MLT to 24 MLT. The EA mostly disappears during the rest of the day. The geomagnetic latitudes and magnetic local times were obtained along each satellite orbit using the quasi-dipole coordinates (Richmond 1995).

4. Seasonal and Local Time Behaviors of the LW-4

In order to observe the LW-4 structure of the EA crests more clearly, we restricted the latitudinal range of the binned TEC data to ±5 ~ 20° MLAT where the anomaly crests normally exist. The data within this latitude range are then averaged for each longitudinal bin and plotted along the geographic longitude as shown in Fig. 2 and Fig. 3 for low and high solar activities, respectively. The longitudinal variations of the averaged TEC (open symbols) for four seasonal cases are presented in 8 local time sectors between 08 MLT and 24 MLT (every two hours) from the top (08 ~ 10 MLT)

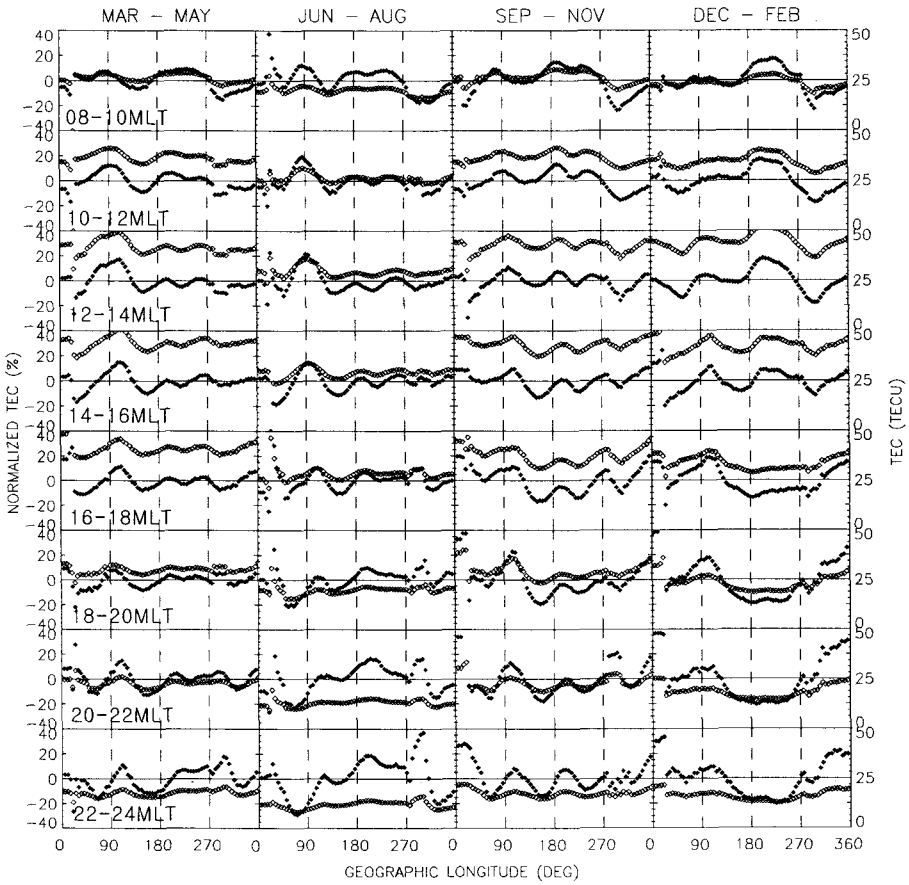

Figure 2. Longitudinal wavenumber-4 (LW-4) structures of the equatorial anomaly crests between 08 MLT and 24 MLT (every two hours) from the top (08~10 MLT) to bottom (22~24 MLT) for four seasonal cases: low solar activity. The open and filled symbols represent the averaged TECs within each bin and the normalized TECs by the longitudinally averaged TEC values, respectively.

to bottom (22 ~ 24 MLT) panels. The TEC values range from 0 to 50 TECU and from 0 to 100 TECU for low and high solar activities, respectively. These figures also include the normalized TEC values (filled symbols) by the longitudinal average values ranging from –40 to +40 for both solar activities. The 5-point running average is applied for these longitudinal plots. The LW-4 structure seems to appear more clearly in the normalized TEC. Note that the noisy parts around the 0 – 40° and 290 – 310° longitude sectors in the line plots are due to the lack of the TOPEX observations in the continental African and South American sectors along the magnetic equator and therefore should be considered with caution.

In Fig. 2 and Fig. 3, the longitudinal variations of the anomaly crests show the largest peak at around 90° GLON for the most of seasons, but particularly during June solstice, and the other three peaks appear at around 200°, 270°, and 360° GLON for both the low and high solar activity conditions. Although it is not regularly distributed in longitude and its amplitude as is assumed in the initial observations of the structure in Sagawa et al. (2005), the patterns of four peaks and valleys are

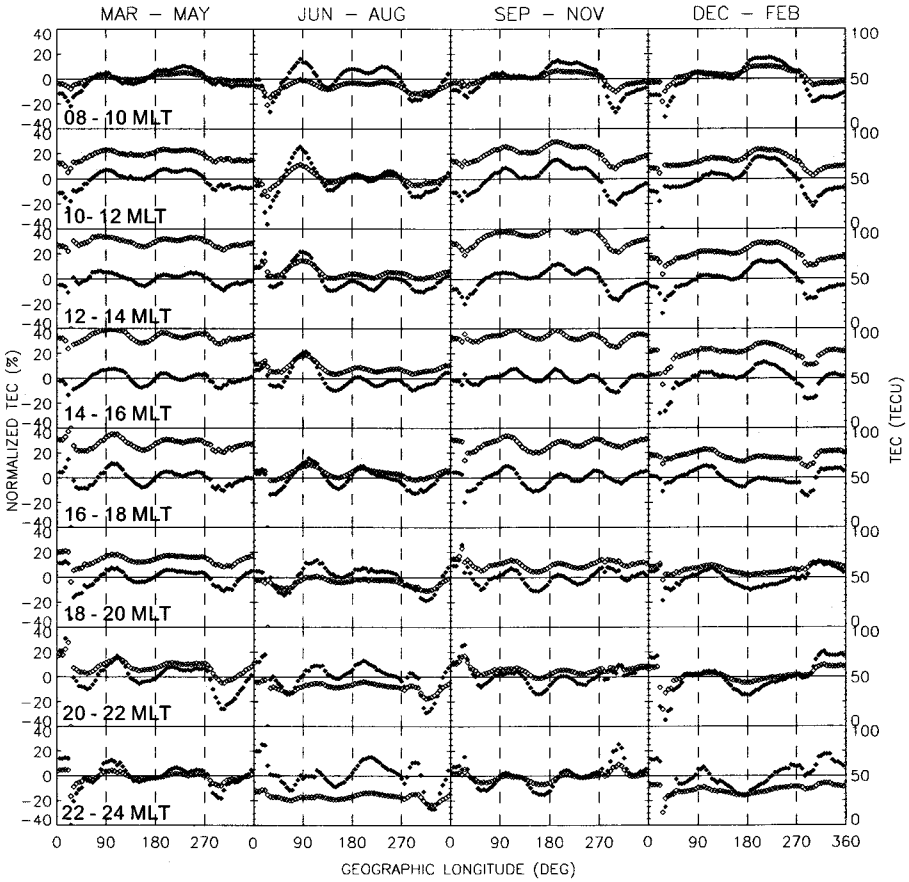

Figure 3. Longitudinal wavenumber-4 (LW-4) structures of the equatorial anomaly crests: high solar activity

considered to be close to the longitudinal wavenumber-4 structure. However, it should be noted that during both low and high solar activities the December solstice case shows only three peaks - that is, the two peaks appeared at 200° GLON and 270° GLON are not separated, but one broad peak exists. And the peak around 90° GLON looks much smaller than the other seasonal cases throughout the morning until 14-16 MLT. The absence of the LW-4 during December solstice was also reported in other studies including Oh (2007) and Scherliess et al. (2008). This will be further discussed later in this study.

Other seasonal characteristics observed in our study is that the LW-4 structures during equinoxes persist until nearly midnight, but the structure during June solstice is maintained only until before the sunset, 16~18MLT in these figures. The daytime LW-4 structures are comparable during both equinoxes and June solstice. The equinoctial LW-4 structure is gradually weakened with the local time after sunset. During June solstice, however, the two peaks located in the pacific sector (200° and 270° GLON) are merged into one large and broad enhancement and the largest one in the Asian sector (90° GLON) is quickly collapsed to be very small compared with the other peaks. As previous studies reported (Sagawa et al. 2005, Scherliess et al. 2008), we also found that the LW-4 tends to

drift, though barely noticeably, eastward near the sunset and during the nighttime.

5. Discussions

The LW-4 structure in the EA crests was not discovered until recently in the ionospheric observations. It does not appear in the global snapshot of the ionosphere such as the Global Ionosphere Map (GIM) based on the GPS measurements, which shows global diurnal variations of the ion densities at a certain universal time, but appears only in a fixed local time frame for the global equatorial ionosphere since its spatial scale and amplitudes are almost comparable to those of the typical diurnal variations of the electron densities. Although the peaks or valleys of the LW-4 are fixed at certain locations, it cannot be distinguished from the diurnal variations of the ionosphere. Therefore it requires extensive space-born observations, which can cover the global ionosphere for a fixed local time sector and become available only in the last decade. Since the first report by Sagawa et al. (2005) from the IMAGE/FUV observation it seems to be reasonably well accepted that the LW-4 originates from the eastward propagating diurnal component of the non-migrating tide with zonal wavenumber-3 (DE3), which is imposed on the background migrating diurnal tide. Diurnal tide is responsible for the regular EA in the ionosphere by inducing the E-region dynamo electric field that maps up to the F-region along the magnetic field lines and produces the $E \times B$ upward ion drift. The additionally imposed non-migrating tidal forcing modulates the dynamo electric field to create the LW-4 structure (Kil et al. 2007).

The LW-4 structure in the ionosphere seems to be basically the result of the coupling between the lower and upper atmospheres, which is, in this case, the E-region dynamo via ion-neutral interactions. The crucial factors for this coupling can be considered to be the tidal forcing from the lower atmosphere and the existence of the ions in the upper atmosphere. Before discussing the association of the LW-4 with the lower atmospheric tidal forcing, we first discuss the effects of the upper atmospheric ion density variations on the LW-4.

5.1 Upper Atmospheric Effects

The upper atmospheric ion density variations may affect the LW-4 structure as ion-neutral interactions are enhanced or reduced. There are various elements influencing ion density variations, internally and externally, but the most important factors in determining the density variations, in particular externally, are the solar and geomagnetic activities. For the solar activity variations of ion densities, Immel et al. (2006) expected the greatest troposphere-ionosphere coupling at the peak of the solar cycle when E-region ion densities are highest, which implies the stronger LW-4 pattern for the solar maximum than for the solar minimum. However, we couldn't find any significant difference in the LW-4 structure between the low and high solar activity conditions. Jee et al. (2004)'s study on the climatology of the ionosphere using the same TOPEX TEC data showed that although the TEC of the EA crest is greatly enhanced from the low to high solar activity conditions, the crest-to-trough ratio along the magnetic equator does not change during the day, indicating that the solar activity hardly affects the strength of the equatorial fountain effect. Similar results were also reported in the observations of the equatorial vertical ion drifts, which showed the negligible variations with solar activity during the day (Scherliess & Fejer 1999). With respect to the geomagnetic activity, it was reported that the LW-4 structure appears not only during geomagnetically quiet condition but also during disturbed condition (Scherliess et al. 2008), which implies the negligible role of the geomagnetic activity in the determination of the LW-4 structure.

The most prominent characteristics of the LW-4 structure in this study are (1) the absence of the LW-4 during December solstice and (2) the sudden collapse of the structure shortly after sunset

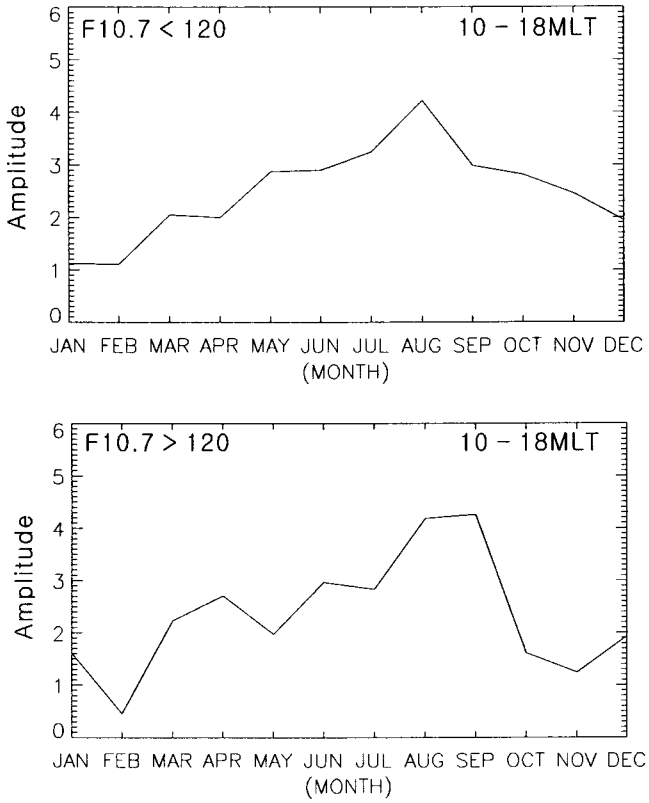

Figure 4. Monthly variations of the amplitudes of the wavenumber-4 component computed from the Fourier analysis of the normalized TECs within $\pm 5 \sim 20^\circ$ MLAT along the longitude in the 10-18 local time sector for low (top) and high (bottom) solar activities.

during June solstice. The second characteristic might be related with the strong seasonal variations of the pre-reversal enhancement (PRE) in the vertical ion drift around sunset. It was observed that the PRE is much stronger during equinoxes/high solar activity than during solstices/low solar activity (Scherliess & Fejer 1999). The strong PRE is able to contribute to maintain the anomaly structure after sunset by lifting the whole structure to the higher altitudes where the recombination becomes slower. In their TOPEX TEC data analysis Jee et al. (2004) observed that the variations of the EA with season and solar activity after sunset were quite different from those variations during the day: after sunset throughout the evening, not only the EA crest densities but also the crest-to-trough ratio are significantly larger during equinoxes/high solar activity than during solstices/low solar activity, which is consistent with the seasonal and solar activity variations of the pre-reversal enhancement (PRE). The seasonal variations of the LW-4 seem to agree with the seasonal behavior of the PRE. However, the LW-4 is nearly independent of the solar activity conditions although the PRE and its effects on the EA are closely related to the solar activity. Furthermore, Kil et al. (2007) reported that the longitudinal morphology of the PRE does not show the LW-4 structure in the observations of the equatorial upward ion drift at 18-19 LT as a representative of the PRE from the first Republic of China Satellite (ROCSAT-1). Therefore, although the PRE greatly affects the EA itself, it does not

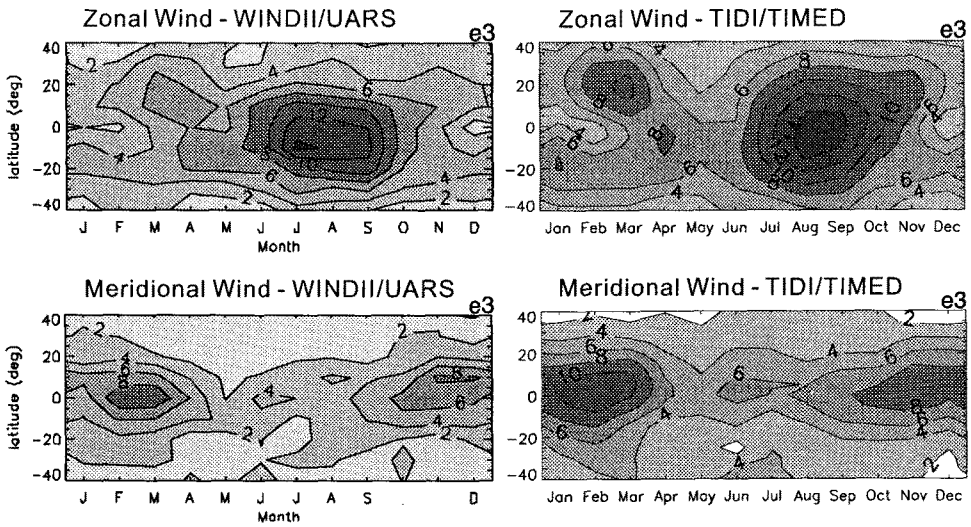

Figure 5. Amplitudes (m/sec) of the eastward propagating zonal wavenumber-3 diurnal tide for the zonal (top) and meridional (bottom) components at 95 km from UARS (HRDI and WINDII, 1991-1994, left) and TIDI (2002-2005, right) from Oberheide et al. (2006).

seem to be contributing to the LW-4 structure of the EA crests.

The LW-4 structure appears to start developing at 10~12 MLT with the formation of the EA, and the structure becomes very clear at 12~14 MLT for most of seasons until it disappears after sunset. If the LW-4 is intimately related to the longitudinal modulation of the equatorial fountain effect, which is driven by E-region dynamo electric field only during the daytime, there would be no driving force for the LW-4 structure during the nighttime. Therefore, once the driving force stops working shortly after sunset, the LW-4 structure will drift with the background plasma drift, which is eastward at night (Fejer et al. 1991). Previous studies reported this eastward drift of the LW-4 structure in their analysis of satellite measurements (Sagawa et al. 2005, Scherliess et al. 2008, Kil et al. 2008). In our study, the eastward drift of the LW-4 after sunset was also observed, but the magnitude of the drift is relatively small, less than 20° in longitude during about 6-hour time period from the sunset to the midnight.

5.2 Lower Atmospheric Effects

In order to observe the correlation between the LW-4 structure and its driving forces in the lower atmosphere, we performed a simple comparison between the monthly variations of the tidal winds and the LW-4 structure. For the representative of the LW-4 monthly variations, we applied the Fourier transform of the normalized TECs within $\pm 5 \sim 20°$ MLAT along the longitude and computed the average amplitudes of the wavenumber-4 component for each month, which is then displayed as a function of month in Fig. 4. We used only the values from 10 to 18 MLT for this analysis because they show clear longitudinal structure during that time.

This figure shows that the wavenumber-4 components for both low and high solar activities are minimized during the December solstice period, as the LW-4 structures in Fig. 2 and Fig. 3 are faded in this period. In order to compare with tidal forcing, we adopted diurnal tidal amplitudes of the meridional and zonal winds from Oberheide et al. (2006). Since the underlying physical source of

the LW-4 is considered to be the eastward propagating diurnal tide with zonal wavenmuber-3 (DE3), we present only this component of the neutral winds in Fig. 5. The displayed are the amplitudes of the zonal (top) and meridional(bottom) winds at 95 km from UARS (HADI and WINDII) (left) and TIMED (TIDI) (right). From the comparison between Fig. 4 and 5, we can find that the monthly variations of the LW-4 are generally similar to that of the zonal wind at low latitudes.

Note that the longitudinal pattern of the EA crests in Fig. 2 and 3 shows the longitudinal wavenumber-4 structure only in the sense that it has four peaks and valleys; it is not regularly spaced with 90° in longitude, and the magnitudes of the peak amplitude are all different. Therefore, it cannot be anticipated that the wavenumber-4 component from the Fourier analysis exactly represents the LW-4 pattern. However, the similarity in monthly variations between the zonal wind and the LW-4 still provides an enough physical insight into why the LW-4 was absent during December solstice. Interestingly, the zonal and meridional winds show different monthly variations in both observations in Fig. 5; while the zonal wind has a maximum around August and minimum around December, the meridional wind shows nearly the opposite as discussed by Oberheide & Forbes (2008). Since the monthly variation of the LW-4 is quite different from that of the meridional wind but generally similar to that of the zonal wind, the latter seems to play a dominant role in the formation of the LW-4 structure in the EA crest. This result may also indicate that although both the zonal and meridional winds in the E-region can contribute to the production of the equatorial eastward electric field that is responsible for the EA in the F-region, the zonal wind seems to have a larger effect than the meridional wind.

6. Conclusions

Due to its spatial or temporal scales that is nearly comparable to the diurnal variations of the plasma density in the global ionosphere, the LW-4 structure was exposed only recently in the various satellite observations. We utilized the TOPEX TEC measurements collected for more than a full solar cycle (from Aug. 1992 to Oct. 2005) to observe the variations of the LW-4 structure in the equatorial anomaly crests with season, local time, and solar activity. Our study shows that the LW-4 structure has clear four peaks at fixed longitude sectors during the daytime for both equinoxes and June solstice. In spite of being called a wavelike structure, however, the magnitudes and spatial intervals of the peaks are far from being the same or regular as shown in Fig. 2 and 3. After sunset, the four-peak structure is gradually weakened during equinoxes and this proceeds much faster during June solstice. Furthermore, the whole structure begins to move eastward, most probably with the background plasma. This indicates that driving force for the LW-4 persists only during the daytime and stops working shortly after sunset. The longitudinal variations during December solstice do not show the LW-4 structure. Especially, two peaks in the Pacific sector are not separated at all and the peak in the Indian sector, typically the largest one in the other seasons, is much smaller throughout the morning until 14-16 MLT. Finally all these features of the LW-4 are almost similar for both low and high solar activity conditions.

There are two fundamental factors that determine the LW-4 structure: the driving forces from the lower atmosphere (probably the non-migrating diurnal tidal forcing) and the ion densities in the upper atmosphere, since the lower atmospheric forcing is fundamentally transferred to the E-region ionosphere via the ion-neutral collision. For the upper atmospheric factor (e.g., ion density), it was found that the LW-4 structure is almost independent of the solar and magnetic activities, implying that the LW-4 seems not to be very sensitive to the ion density variations on which the solar and magnetic activities cause significant effects. However, the LW-4 structure seems to be closely related with the lower atmospheric tidal winds as is indicated in our observation that the seasonal variations

of the LW-4 structure are consistent with the monthly variations of the wavenumber-3 component of the zonal winds. Therefore, it seems to be very reasonable to assume that the lower atmospheric tidal forcing derives the LW-4 structure by modulating the E×B ion drift.

Acknowledgements: We thank L. Scherliess for providing the TOPEX TEC data that is originally obtained from the Physical Oceanography Distributed Active Center (PO.DAAC) at JPL/NASA. This work was supported by Korea Science and Engineering Foundation grant (No. R01-2006-0000-11003-0). G. Jee acknowledges support from the Korea Polar Research Institute (KOPRI) through the COMposition of Polar Atmosphere and Climate Change (PE08030).

References

Codrescu, M. V., Beierle, L. K., Fuller-Rowell, T. J., Palo, S. E., & Zhang, X. 2001, Radio Sciences, 36, 325

Codrescu, M. V., Palo, S. E., Zhang, X., Fuller-Rowell, T. J., & Poppe, C. 1999, J. of Atmospheric and Solar-Terrestrial Physics, 61, 281

England, S. L., Immel, T. J., Sagawa, E., Henderson, S. B., Hagan, M. E., Mende, S. B., Frey, H. U., Swenson, C. M., & Paxton, L. J. 2006a, JGR, 111, doi:10.1029/2006JA011795

England, S. L., Maus, S., Immel, T. J., & Mende, S. B. 2006b, GRL, 33, doi:10.1029/2006GL027465

Fejer, B. G., de Paula, E. R., Gonzalez, S. A., & Woodman, R. F. 1991, JGR, 96, 13901

Forbes, J. M., Revelle, D., Zhang, X., & Markin, R. E. 1996, JGR, 103, 7293

Forbes, J. M., Russell, J., Miyahara, S., Zhang, X., Palo, S., Mlynczak, M., Mertens, C. J., & Hagan, M. E. 2006, JGR, 111, doi:10.1029/2005JA011492

Fu, L. L., Christensen, E. J., & Yamarone Jr., C. A. 1994, JGR, 99, 24369

Hartman, W. A. & Heelis, R. A. 2007, JGR, 112, doi:10.1029/2006JA011773

Ho, C. M., Wilson, B. D., Mannucci, A. J., Lindqwister, U. J., & Yuan, D. N. 1997, Radio Sciences, 32, 1499

Horvath, I. 2006, JGR, 111, doi:10.1029/2006JA011679

Immel, T. J., Sagawa, E., England, S. L., Henderson, S. B., Hagan, M. E., Mende, S. B., Fery, H. U., Swenson, C. M., & Paxton, L. J. 2006, GRL, 33, doi:10.1029/2006GL026161

Jee, G., Schunk, R. W., & Scherliess, L. 2004, JGR, 109, doi:10.1029/2003JA010058

Jee, G., Schunk, R. W., & Scherliess, L. 2005, J. of Atmospheric and Solar-Terrestrial Physics, 67, 365

Kil, H., Oh, S.-J., Kelley, M. C., Paxton, L. J., England, S. L., Talaat, E., Min, K.-W., & Su, S.-Y. 2007, GRL, 34, doi:10.1029/2007GL030018

Kil, H., Talaat, E. R., Oh, S.-J., Paxton, L. J., England, S. L., & Su, S.-Y., 2008, JGR, 113, doi:10.1029/2008JA013106

Lin, C. H., Wang, W., Hagan, M. E., Hsiao, C. C., Immel, T. J., Hsu, M. L., Liu, J. Y., Paxton, L. J., Fang, T. W., & Liu, C. H. 2007, GRL, 34, doi:10.1029/2007GL029265

Lynn, K. J. W., Sjarifudin, M., Harris, T. J., & Le Huy, M. 2004, Annales. Geophysicae, 22, 2837

Oberheide, J. & Forbes, J. M. 2008, GRL, 35, doi:10.1029/2007GL032397

Oberheide, J., Wu, Q., Killeen, T. L., Hagan, M. E., & Roble, R. G. 2006, JGR, 111, doi:10.1029/2005JA011491

Oh, S.-J. 2007, Ph.D. dissertation, Seoul National University

Richmond, A. D. 1995, Journal of Geomagnetism and Geoelectricity, 47, 191

Sagawa, E., Immel, T. J., Frey, H. U., & Mende, S. B. 2005, JGR, 110, doi:10.1029/2004JA010848

Scherliess, L. & Fejer, B. G. 1999, JGR, 104, 6829

Scherliess, L., Thompson, D. C., & Schunk, R. W. 2008, JGR, 113, doi:10.1029/2007JA012480
Vladimer, J. A., Jastrezebski, P., Lee, M. C., Doherty, P. H., Decker, D. T., & Anderson, D. N. 1999, Radio Sciences, 34, 1239
Zhang, X., Forbes, J. M., Hagan, M. E., Russell III, J. M., Palo, S. E., Mertens, C. J., & Mlynczak, M. G. 2006, JGR, 111, doi:10.1029/2005JA011504
Zhu, L., Schunk, R. W., Jee, G., Scherliess, L., Sojka, J. J., & Thompson, D. C. 2006, Radio Sciences, 41, doi:10.1029/2005RS003336